Proc. Natl. Acad. Sci. USA
Vol. 76, No. 7, pp. 3046–3050, July 1979
Chemistry

Time-resolved resonance Raman spectroscopy of intermediates of bacteriorhodopsin: The bK_{590} intermediate

(purple membrane/kinetics/batho-intermediate/prelumi-bacteriorhodopsin/Raman microbeam)

JAMES TERNER, CHUNG-LU HSIEH, A. R. BURNS, AND M. A. EL-SAYED*

Department of Chemistry, University of California, Los Angeles, California 90024

Communicated by Howard Reiss, March 26, 1979

ABSTRACT **We have combined microbeam and flow techniques with computer subtraction methods to obtain the resonance Raman spectrum of the short lived batho-intermediate (bK_{590}) of bacteriorhodopsin. Comparison of the spectra obtained in ^1H_2O and ^2H_2O, as well as the fact that the bK_{590} intermediate shows large optical red shifts, suggests that the Schiff base linkage of this intermediate is protonated. The fingerprint region of the spectrum of bK_{590}, sensitive to the isomeric configuration of the retinal chromophore, does not resemble the corresponding region of the parent bR_{570} form. The resonance Raman spectrum of bK_{590} as well as the spectra of all of the other main intermediates in the photoreaction cycle of bacteriorhodopsin are discussed and compared with resonance Raman spectra of published model compounds.**

Bacteriorhodopsin, a retinal–protein complex similar in structure to the visual pigments (1), converts light into chemical energy (2). Bacteriorhodopsin is thought to operate as a proton pump, producing an electrochemical gradient across the bacterial cell membrane, which drives the synthesis of ATP (3), according to the chemosmotic theory of Mitchell (4).

The intermediates of bacteriorhodopsin, extensively characterized by flash photolytic techniques (5), are now being investigated by resonance Raman spectroscopy to obtain detailed vibrational information about the retinal chromophore (6–9). Most recently, *time-resolved* resonance Raman spectroscopy using pulsed laser (10–13) and flow techniques (14–17) has produced complete spectra of bR^{DA}_{560} (13, 16, 17) and its component isomers (17) bL_{550} (17), bM_{412} (11, 15, 16), and bO_{640} (unpublished data), although not all points are presently agreed upon by the various authors. In the study described here, we modified a previously described flow technique (17) by tightly focusing a continuous wave (cw) laser beam to obtain finer time resolution in order to minimize the Raman scattering from intermediates formed subsequent to bK_{590}. The bK_{590} spectrum shown in this paper was obtained at ambient temperature and is different from a spectrum obtained recently (16) at 77 K. In the final section of this paper we compare the resonance Raman spectra of the various species in the bacteriorhodopsin photoreaction cycle.

MATERIALS AND METHODS

Purple membrane was isolated by the method of Becher and Cassim (18) from an S-9 culture of *Halobacterium halobium*, the gift of W. Stoeckenius. The carotenoid content of the purified samples was decreased by photooxidation until the carotenoid bands at 1255 and 1515 cm^{-1} were no longer detectable. The samples were suspended at 50 μM in deionized ^1H_2O or ^2H_2O.

The method used to obtain the resonance Raman spectrum of bK_{590} involves focusing a cw laser beam to a microscopic spot on a rapidly flowing sample jet stream (Fig. 1). The microbeam technique is similar to that used by Berns (19) to achieve high-power densities over microscopic areas. Laser excitation was focused by a microscope objective to give a beam diameter of one micrometer. The beam was focused across the diameter of a vertically flowing jet stream of bacteriorhodopsin. Forcing the sample through a 30-gauge syringe needle (inside diameter, 150 μm) at a flow rate of 0.3 ml/sec gave a stream velocity of 20 m/sec. We estimate that the interaction time of the flowing sample with the focused laser excitation was less than 100 nsec. This procedure is identical to that previously used in this laboratory to obtain the spectrum of bL_{550} (17), except that the interaction time has been decreased from 10 μsec to <100 nsec to minimize the appearance of bL_{550}. The sample reservoir was kept light adapted with a flashlight.

The excitation sources were a Spectra-Physics model 171 krypton ion laser at 5682 Å and a Spectra-Physics model 375 dye laser (rhodamine 560, Exciton) pumped by a Spectra-Physics model 171 argon-ion laser. A fine etalon narrowed the dye laser output to 0.5 Å. Laser power was measured at the sample. Scattered light was collected at 90° and focused onto the slit of a Spex 1870 spectrograph. A filter (Corning 2-63 at

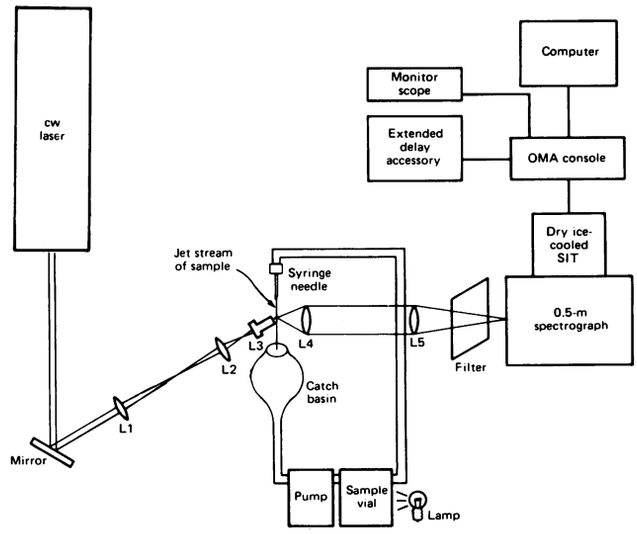

FIG. 1. Experimental arrangement for the resonance Raman microbeam flow experiment. Details are given in the text. L_1, 30-cm f/15 lens; L_2, 6-cm f/3 lens; L_3, Zeiss Neofluar ×40 microscope objective; L_4, 50-mm f/1.2 Canon lens; L_5, 16-cm f/4 lens; OMA, optical multichannel analyzer.

The publication costs of this article were defrayed in part by page charge payment. This article must therefore be hereby marked "*advertisement*" in accordance with 18 U. S. C. §1734 solely to indicate this fact.

Abbreviation: cw, continuous wave.

* To whom correspondence should be addressed.

5682 Å, Corning 3-66 at 5520 Å) was used to attenuate Rayleigh scattering. Our optical multichannel analyzer (Princeton Applied Research Corp., Princeton, NJ) detection system and its operation has been described (17).

To acquire the resonance Raman spectrum of bK_{590}, a spectrum of bK_{590} superimposed upon that of bR_{570} was obtained by using sufficient laser power. By decreasing the laser power, a second spectrum of pure unphotolyzed bR_{570} was obtained and was computer subtracted from the first spectrum to yield the resonance Raman spectrum of bK_{590}. It was not possible to obtain a spectrum of pure bK_{590} without resorting to computer subtraction for two reasons. The maximal amount of conversion of bR_{570} to bK_{590} is 0.3 (20) and, second, it was not possible to enhance bK_{590} vibrations selectively over those of bR_{570} because of interference of the high-energy tail of the intrinsic fluorescence near 6050 Å.

Our computer subtraction procedure and a discussion of the problems involved has been described (17). We show a series of subtractions by a series of arbitrary weighting factors, for the purposes of clarity and to avoid inaccurate normalization. These weighting factors depend only on signal intensity and length of scan and they contain no quantitative information. Oversubtractions, which result in negative peaks, have been eliminated. We have chosen the 1351 and 1643 cm^{-1} bands as internal standards to assist in our normalization procedure. These bands appear to be unique to the spectrum of bR_{570}; they are absent in bK_{590}. None of the spectra shown in this paper has been smoothed. Absolute vibrational frequencies are accurate to ±5 cm^{-1}.

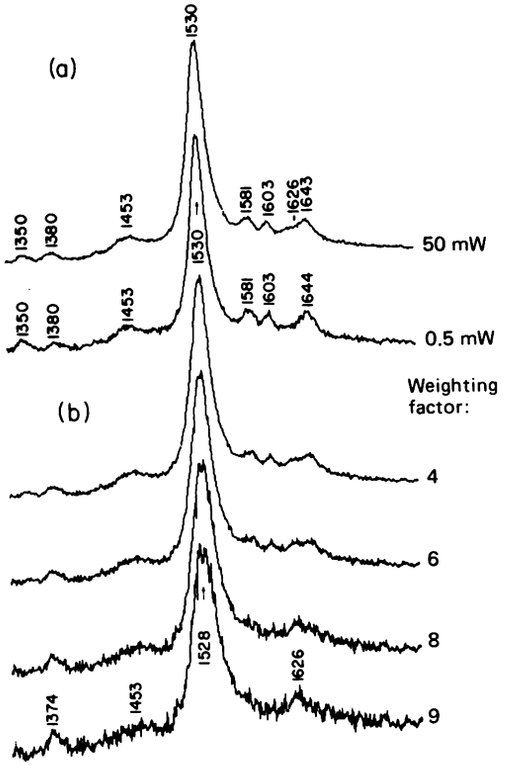

FIG. 2. (*a*) Resonance Raman microbeam flow spectra in the 1350 to 1700 cm^{-1} region, with 5523 Å excitation and a 100-nsec residence time. The high-power spectrum contains the resonance Raman spectrum of bK_{590} superimposed upon that of bR_{570}. The low-power spectrum is the resonance Raman spectrum of unphotolyzed bR_{570}. (*b*) Computer subtraction of the low-power spectrum from the high-power spectrum shown in *a* by a series of arbitrary unnormalized weighting factors to reveal the resonance Raman spectrum of bK_{590} in the 1350 to 1700 cm^{-1} vibrational region.

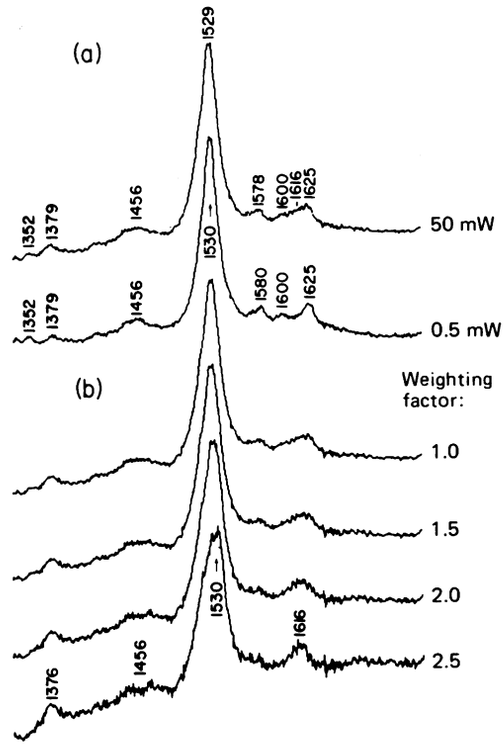

FIG. 3. Repetition of the experiment shown in Fig. 2 for a ^2H_2O suspension, with 5682 Å excitation. Note that the protonated C=N vibration of bR_{570} (*a*) has shifted to 1625 cm^{-1} from 1644 cm^{-1}, and the protonated C=N vibration of bK_{590} (*b*) has shifted to 1616 cm^{-1} from 1626 cm^{-1}.

RESULTS

The 1350 to 1800 cm^{-1} Vibrational Region. This region is important because it contains the ethylenic stretching bands (1510–1580 cm^{-1}) and the deuteration sensitive (6, 21) C=N vibrations (1610–1660 cm^{-1}) (22). The resonance Raman spectra of this vibrational region for the bK_{590} intermediate are shown in Fig. 2. The 1350 cm^{-1} band, which belongs to bR_{570} only, has been used to aid in the normalization. Use of larger weighting factors than those shown results in negative peaks. From Fig. 2*b* it can be seen that bK_{590} possesses a C=C stretch at 1528 cm^{-1}. This peak position varied from 1524 to 1530 cm^{-1} depending on our success at eliminating bL_{550} (excitation is at the λ_{max} of bL_{550}) from our spectra. Other bK_{590} bands at 1626, 1374, and 1453 cm^{-1} also were observed.

The 1626 cm^{-1} band of bK_{590} was determined to be a C=NH^+ stretch by a deuteration experiment (Fig. 3). In the low-power spectrum of Fig. 3*a*, it can be seen that the 1644 cm^{-1} protonated C=N stretch of bR_{570} underwent a deuteration shift to 1625 cm^{-1} as described by Lewis *et al.* (6). The corresponding vibration of bK_{590} at 1626 cm^{-1} also displayed a deuteration shift. The 1626 cm^{-1} vibration in H_2O suspension (Fig. 2*b*) shifted to 1616 cm^{-1} upon suspension of the purple membrane in ^2H_2O (Fig. 3*b*). The data together with the fact that the retinal absorption of bK_{590} exhibits a large red shift (23) suggest that the Schiff base linkage of bK_{590} is protonated.

The 1150 to 1400 cm^{-1} Vibrational Region. The region from 1150 to 1400 cm^{-1}, the so-called fingerprint region, has been shown to be sensitive to the isomeric configuration of the retinals (24). The fingerprint region of bK_{590} derived in Fig. 4, by the method described above, shows bands at 1298, 1328, and 1370 cm^{-1}, which are also common to the bL_{550} (17), bM_{412} (11, 15), and bO_{640} (Fig. 7) intermediates. A large feature, at 1193 cm^{-1}, corresponds to a similar feature of the bL_{550} intermediate. Also present is a band at 1158 cm^{-1}. A band at 1207

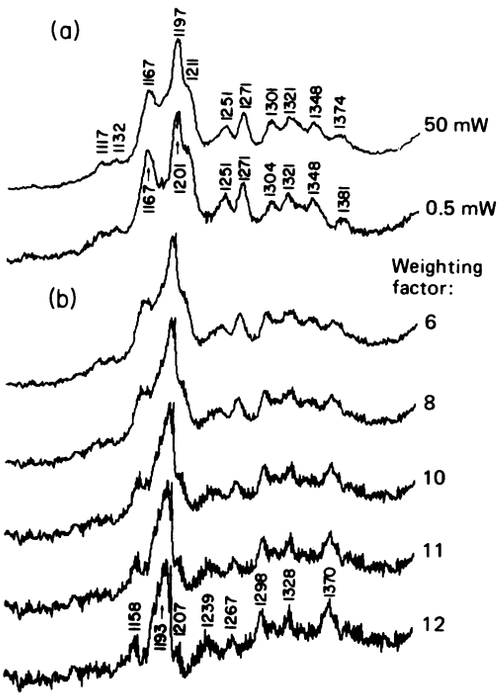

FIG. 4. (*a*) Resonance Raman microbeam flow spectra in the 1100 to 1400 cm^{-1} (fingerprint) region, with 5523 Å excitation and a 100-nsec residence time. The high-power spectrum contains the resonance Raman spectrum of bK_{590} superimposed on that of bR_{570}. The low-power spectrum is the resonance Raman spectrum of unphotolyzed bR_{570}. (*b*) Computer subtraction of the low-power spectrum from the high-power spectrum shown in *a* by a series of unnormalized arbitrary weighting factors to obtain the fingerprint region of the resonance Raman spectrum of bK_{590}. Suspension of the purple membrane in ^2H_2O did not show any new features in this vibrational region. The oversubtracted spectrum (weighting factor = 12) indicates that the peaks at 1158 and 1207 cm^{-1} belong to the spectrum of bK_{590} and are not residuals of the 1167 and 1211 cm^{-1} bands of bR_{570}.

cm^{-1} appears to be a part of the resonance Raman spectrum of the bK_{590} intermediate. Identical results are obtained with the purple membrane suspended in ^2H_2O (25).

The 800 to 1200 cm^{-1} Region. This region contains the carbon-methyl vibration at 1011 cm^{-1} (24) and a region between 800 and 1000 cm^{-1} that is sensitive to suspension of the purple membrane in ^2H_2O (Figs. 5 and 6). Intense bands have been reported in the 800–1000 cm^{-1} region of bathorhodopsin (22, 26) that are not found in model compounds. Although features as intense as those bathorhodopsin bands are not found in bathobacteriorhodopsin (bK_{590}), there are features between 950 and 1020 cm^{-1} that are possibly analogous. In Fig. 5*b* it can be seen that the 1010 cm^{-1} carbon-methyl stretch does not possess the intensity seen in other intermediates (Fig. 7), and prominent features are seen at 968 and 984 cm^{-1}.

When purple membrane is suspended in ^2H_2O, we have found that each form of bacteriorhodopsin possessing a protonated Schiff base at the chromophore displays a unique "deuteration fingerprint" in the region 960 to 1000 cm^{-1} (17). The bK_{590} spectrum also displays a unique pattern in this region. In Fig. 6*b* it can be seen that the 984 cm^{-1} band in ^1H_2O has shifted to either 968 or 1012 cm^{-1} in ^2H_2O, confirming the interaction of a photolabile proton with the chromophore. The pattern in Fig. 6*b* is also different from the deuteration bands of the other intermediates (17), serving to confirm that the resonance Raman spectrum we have observed of bK_{590} is different from that of bO_{640} (25) and bL_{550} (17). We have not been able to observe other bands attributable to bK_{590} between 750 and 968 cm^{-1}. We cannot record bands below 750 cm^{-1} because of the limits of our present detection system.

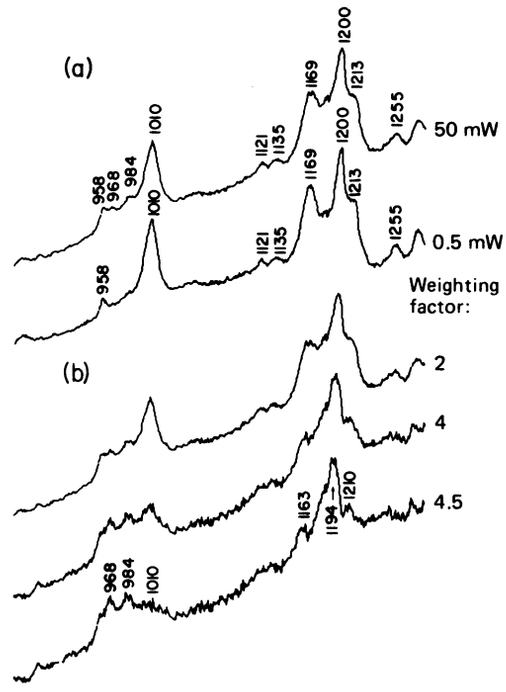

FIG. 5. (*a*) Resonance Raman microbeam flow spectra for the 900 to 1250 cm^{-1} region, with 5682 Å excitation and a 100-nsec residence time. The high-power spectrum contains the resonance Raman spectrum of bK_{590} superimposed upon the spectrum of bR_{570}. The low-power resonance Raman spectrum is unphotolyzed bR_{570}. (*b*) Computer subtraction of the low-power spectrum from the high-power spectrum of *a* by arbitrary unnormalized weighting factors, leaving the resonance Raman spectrum of bK_{590} for the 900 to 1250 cm^{-1} region. The spectrum with weighting factor = 4 may be the correct one. The spectrum with weighting factor = 4.5 is probably oversubtracted.

DISCUSSION

We have concluded that bK_{590} possesses a protonated Schiff base, because a band at 1626 cm^{-1} shifts to 1616 cm^{-1} when the purple membrane is suspended in ^2H_2O. Additionally, a shift of the 984 cm^{-1} band to 968 or 1012 cm^{-1} in ^2H_2O con-

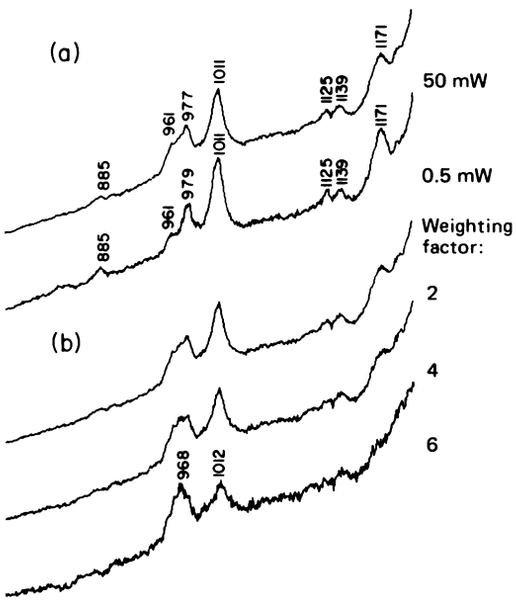

FIG. 6. Repetition of the experiment shown in Fig. 5, with a ^2H_2O suspension. Note that the 984 cm^{-1} band of bK_{590} in H_2O (Fig. 5*b*) has shifted to either 968 or 1012 cm^{-1}.

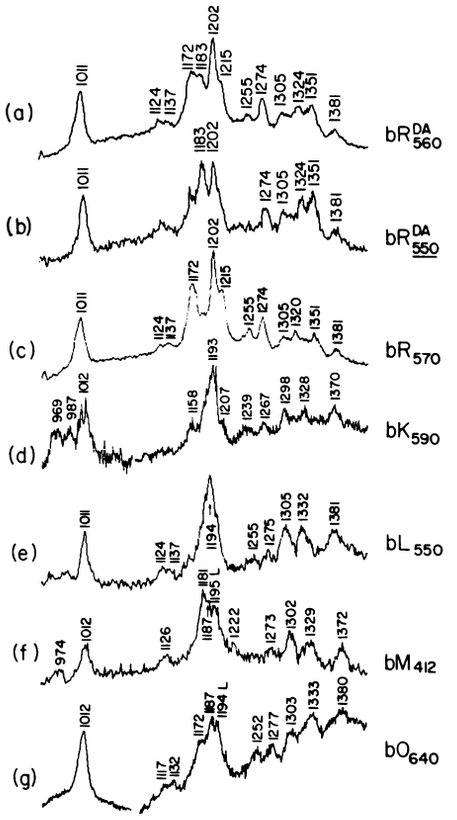

FIG. 7. The fingerprint regions of the resonance Raman spectra of bacteriorhodopsin forms. Curves: a, bR^{DA}_{560} obtained by a dark-adapted recirculating flow experiment (13, 17); excitation at 5145 Å. b, On the assumption that one of the two isomers present in bR^{DA}_{560} is identical to that of bR_{570}, the resonance Raman spectrum of bR_{570} was subtracted from that of bR^{DA}_{560}, leaving the resonance Raman spectrum of the second of the two isomers bR^{DA}_{550} (17); excitation at 5145 Å. c, Unphotolyzed bR_{570} obtained by a low-power light-adapted recirculating flow experiment (13, 17); excitation at 5145 Å. d, bK_{590} obtained by the microbeam flow technique (this paper) and computer subtraction; excitation at 5523 Å. e, bL_{550} obtained by the power-dependent flow technique (17) and computer subtraction; excitation at 5145 Å. f, bM_{412} obtained by a pulsed laser technique and computer subtraction (11, 25); excitation at 4765 Å. The band labeled L is due to bL_{550} although there may be a contribution from bM_{412} underneath. g, bO_{640} obtained by a pulsed laser technique and computer subtraction; excitation at 5520 Å (34).

firms the existence of a photolabile proton coupled to the chromophore. Eyring and Mathies (26) have reported that the Schiff base of bathorhodopsin is protonated, but they noted no net change in the bond order of the C=NH$^+$ bond on going from rhodopsin to bathorhodopsin. On the other hand, we have noted a significant change in the C=NH$^+$ frequency on going from bR_{570} (1644 cm^{-1}) to bK_{590} (1626 cm^{-1}). It was proposed (27) that in the latter a strong hydrogen bonding between the Schiff base proton and the protein might explain the relatively low C=N frequency observed for this system. If the strength of the hydrogen bonding increases in the bK_{590} intermediate, a further decrease in the C=N frequency to the observed 1626 cm^{-1} might be expected. We have observed that the lower the C=NH$^+$ frequency, the smaller the deuteration shift. This might be accounted for by the fact that the stronger the hydrogen bonding to the protein, the weaker the N—H bonding becomes and thus its effect on the vibration of the neighboring C=N group lessens.

Recent picosecond absorption studies on rhodopsin (28) and bacteriorhodopsin (29) have shown evidence for a proton tunneling phenomenon, with a pronounced deuteration effect in the step leading to the first intermediate of these pigments. It is difficult to say whether the proposed change in force constant of the N—H bond on going from the bR_{570} to the bK_{590} is sufficient to explain the picosecond results. However, the fact that proton tunneling was also observed in rhodopsin which shows no change in C=N vibration frequency upon changing to bathorhodopsin might shed doubt about the correlation of proton tunneling and the deuteration effect in the picosecond studies.

Table 1. Deuteration effects on bacteriorhodopsin vibrations (cm^{-1})

Intermediate	Schiff base vibrations ^1H_2O	Schiff base vibrations ^2H_2O	800 to 1050 cm^{-1} region ^1H_2O	800 to 1050 cm^{-1} region ^2H_2O	Schiff base
bR^{DA}_{560}	1644	1622	1012	991	Protonated
			1012	979	
			807	815	
bR^{DA}_{550}	1644	1622	1012	991	Protonated
			807	815	
bR_{570}	1644	1622	1012	979	Protonated
bK_{590}	1626	1616	984	968 or 1012	Protonated
bL_{550}	1647	1619	?	988	Protonated
bM_{412}	1623	1620	No effects		Not protonated
bO_{640}	1630	1616	?	992	Protonated
			?	965	
			?	947	

The fingerprint region (1100 to 1400 cm^{-1}) has been shown to be sensitive to the isomeric configuration of the various retinals (22). It is difficult to match the fingerprint region of bK_{590} with published model compounds; however, there appears to be a resemblance to a protonated Schiff base of all-*trans* retinal (30). The peaks of bK_{590} at 1158, 1193, 1239, and 1267 cm^{-1} could correspond to peaks of the all-*trans* model at 1165, 1198, 1240, and 1275 cm^{-1} (30).

Because the complete spectra of the main intermediates in the bacteriorhodopsin cycle have been obtained (11, 13, 17), it is appropriate to summarize and discuss our results. Bacteriorhodopsin Schiff base C=NH$^+$ frequencies are listed in Table 1. The bM_{412} intermediate was the only intermediate that did not exhibit an observable deuteration shift of the Schiff base C=N vibration, thus implying that only bM_{412} possesses an unprotonated Schiff base. Also, all forms listed except bM_{412} exhibited deuteration shifts in the 800 to 1050 cm^{-1} region, confirming that bM_{412} is the only intermediate that does not possess a photolabile proton coupled to the chromophore. Deprotonation of the Schiff base is thus concluded to be the $bL_{550} \rightarrow bM_{412}$ step. The reprotonation step is $bM_{412} \rightarrow bO_{640}$ (25).

The fingerprint regions of the bacteriorhodopsin forms in Fig. 7 show that bands at 1274, 1305, 1324, and 1381 cm^{-1} are common to all bacteriorhodopsin forms with slight shifts in frequency. There is general agreement that there is an isomeric change going on from bR^{DA}_{560} to bR_{570}, (31, 32), and it is likely that an isomeric change may occur on going from bR_{570} to the photoinduced intermediates (11, 15, 32). This would suggest that the bands at 1274, 1305, 1324, and 1381 cm^{-1} are not valid indicators of the isomeric configuration of the bacteriorhodopsin chromophore.

The remaining bands of the fingerprint region from 1000 to 1250 cm^{-1} might provide some insight into possible conformational changes of retinal during the photoreaction process.

The dissimilarity of bR_{550}^{DA} (1183 and 1202 cm^{-1}) and bR_{570} (1172, 1202, and 1215 cm^{-1}) appears to confirm an isomeric change (17, 31, 32). Additionally, the dissimilarity between the 1172, 1202, and 1215 cm^{-1} bands of bR_{570} and the large 1193 cm^{-1} band and smaller bands at 1158 and 1207 cm^{-1} of bK_{590} might imply a conformational change of the retinal chromophore on going from bR_{570} to bK_{590}. It is interesting to note the overall similarity of the fingerprint regions of bK_{590}, bL_{550}, and bM_{412} and their marked dissimilarity to bR_{570}. It must be remembered, however, that all these spectra, except those for bR_{570} and bR_{560}^{DA}, are obtained by subtraction techniques, with the problems these techniques entail. Comparison with model compounds must thus be made with caution, particularly when it is not known how the large red shift experienced by most bacteriorhodopsin intermediates is manifested in the resonance Raman spectrum or upon the isomeric configuration of the retinal chromophore. Now that detailed resonance Raman spectra of the various bacteriorhodopsin intermediates are available, modeling (33), solvent studies, and theoretical studies should soon provide insight into the mechanism of the bacteriorhodopsin proton-pumping process.

Note Added in Proof. The resonance Raman data for the bO_{640} intermediate quoted in this paper are from ref. 34.

The authors are grateful to Prof. W. Stoeckenius for the sample, to Profs. M. Nicol and P. Boyer for the use of their facilities, and to M. Berns for lending us the microscope lenses. We thank Drs. G. Eyring and R. Mathies for a preprint of their manuscript prior to publication. J.T. acknowledges a National Science Foundation National Needs Traineeship. This work was supported by the U.S. Department of Energy, Office of Basic Energy Sciences.

1. Oesterhelt, D. & Stoeckenius, W. (1971) *Nature (London) New Biol.* **233,** 149–152.
2. Oesterhelt, D. & Stoeckenius, W. (1973) *Proc. Nat. Acad. Sci. USA* **70,** 2853–2857.
3. Racker, E. & Stoeckenius, W. (1974) *J. Biol. Chem.* **249,** 662–663.
4. Mitchell, P. (1966) *Biol. Rev. Cambridge Philos. Soc.* **41,** 445–502.
5. Stoeckenius, W., Lozier, R. H. & Bogomolni, R. A. (1979) *Biochim. Biophys. Acta* **505,** 215–278.
6. Lewis, A., Spoonhower, J., Bogomolni, R. A., Lozier, R. H. & Stoeckenius, A. (1974) *Proc. Natl. Acad. Sci. USA* **71,** 4462–4466.
7. Mendelsohn, R. (1973) *Nature (London)* **243,** 22–24.
8. Mendelsohn, R., Verma, A. L., Bernstein, H. J. & Kates, M. (1974) *Can. J. Biochem.* **52,** 774–781.
9. Mendelsohn, R. (1976) *Biochim. Biophys. Acta* **427,** 295–301.
10. Campion, A., Terner, J. & El-Sayed, M. A. (1977) *Nature (London)* **265,** 659–661.
11. Terner, J., Campion, A. & El-Sayed, M. A. (1977) *Proc. Natl. Acad. Sci. USA* **74,** 5212–5216.
12. Campion, A., El-Sayed, M. A. & Terner, J. (1977) *Biophys. J.* **20,** 369–375.
13. Terner, J. & El-Sayed, M. A. (1978) *Biophys. J.* **24,** 262–264.
14. Marcus, M. A. & Lewis, A. (1977) *Science* **195,** 1328–1330.
15. Aton, B., Doukas, A. G., Callender, R. H., Becher, B. & Ebrey, T. G. (1977) *Biochemistry* **16,** 2995–2999.
16. Marcus, M. A. & Lewis, A. (1978) *Biochemistry* **17,** 4722–4735.
17. Terner, J., Hsieh, C.-L. & El-Sayed, M. A. (1979) *Biophys. J.* **26,** 527–542.
18. Becher, B. M. & Cassim, J. Y. (1975) *Prep. Biochem.* **5,** 161–178.
19. Berns, M. W. (1971) *Exp. Cell Res.* **65,** 470–473.
20. Goldschmidt, C. R., Ottolenghi, M. & Korenstein, R. (1976) *Biophys. J.* **16,** 839–843.
21. Oseroff, A. R. & Callender, R. H. (1974) *Biochemistry* **13,** 4243–4248.
22. Heyde, M. E., Gill, D., Kilponen, R. G. & Rimai, L. (1971) *J. Am. Chem. Soc.* **93,** 6776–6780.
23. Honig, B., Greenberg, A. D., Dinur, U. & Ebrey, T. G. (1976) *Biochemistry* **15,** 4593–4599.
24. Rimai, L., Gill, D. & Parsons, J. L. (1971) *J. Am. Chem. Soc.* **93,** 1353–1357.
25. Terner, J. (1979) Dissertation (Univ. of California, Los Angeles).
26. Eyring, G. & Mathies, R. (1979) *Proc. Natl. Acad. Sci. USA* **76,** 33–37.
27. Lewis, A., Marcus, M. A., Ehrenberg, B. & Crespi, H. (1978) *Proc. Natl. Acad. Sci. USA* **75,** 4642–4646.
28. Peters, K., Applebury, M. L. & Rentzepis, P. M. (1977) *Proc. Natl. Acad. Sci. USA* **24,** 3119–3123.
29. Applebury, M. L., Peters, K. & Rentzepis, P. M. (1978) *Biophys. J.* **23,** 375–382.
30. Mathies, R., Freedman, T. B. & Stryer, L. (1977) *J. Mol. Biol.* **109,** 367–372.
31. Sperling, W., Carl, P., Rafferty, Ch. N. & Dencher, N. A. (1977) *Biophys. Struct. Mechanism* **3,** 79–94.
32. Pettei, M. J., Yudd, A. P., Nakanishi, K., Henselman, R. & Stoeckenius, W. (1977) *Biochemistry* **16,** 1955–1959.
33. Warshel, A. (1979) *Photochem. Photobiol.*, in press.
34. Terner, J., Hsieh, C.-L., Burns, A. R. & El-Sayed, M. A. (1979) *Biochemistry,* in press.